Electronic Supplementary Information

Electron Spin Polarization Generated by Transport of Singlet and Quintet Multiexcitons to Spin-Correlated Triplet Pairs during Singlet Fissions

Saki Matsuda[‡], *Shinya Oyama*[‡] and *Yasuhiro Kobori*[†, ‡, *]

[‡] Department of Chemistry, Graduate School of Science, Kobe University, 1–1 Rokkodai–cho, Nada–ku, Kobe 657–8501, Japan

[†] Molecular Photoscience Research Center, Kobe University, 1–1 Rokkodai–cho, Nada–ku, Kobe 657–8501, Japan

[*] Corresponding Author: ykobori@kitty.kobe-u.ac.jp

1. Samples

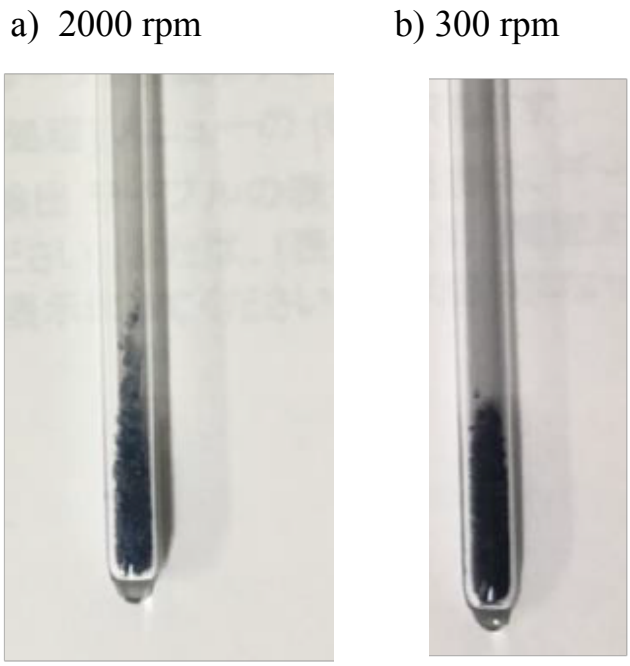

Fig. S1. Photos of 5 mm diameter EPR tubes containing many small films cut from the fabricated 1 cm^2 films. Many small cut pieces were required to ensure the optical densities c.a. 1 by the 532 nm lasers and powder-pattern EPR analyses for the fabricated thin films, because laser irradiation spot area was c.a. 10 mm^2 which is much larger than the sizes of the crashed film.

2. EPR line-shape contributions by the TT → T+T jump dissociation model for the T+T state.

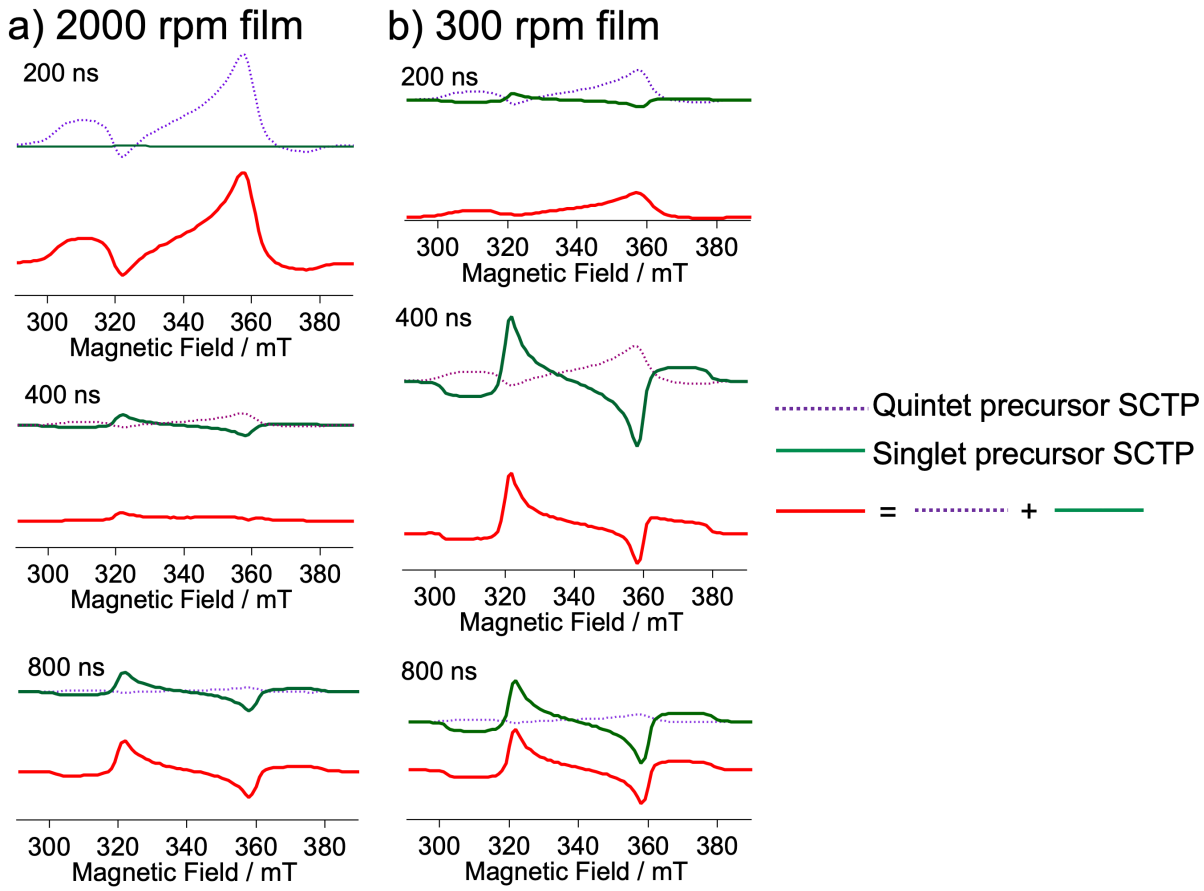

Fig. S2. Purple dotted lines and green solid lines are computed TREPR spectra in Fig. 5c and in Fig. 5b, as the quintet precursor SCTP and the singlet precursor SCTP, respectively for the films spun at a) 2000 rpm and b) 300 rpm. For each delay time (200, 400, 800 ns), intensity contributions from the quintet (A/E/A/E) and singlet (E/A/E/A) precursors are presented to obtain the red spectrum by the sum of the purple and green lines. The red spectra correspond to the red lines as the simulated EPR spectra in Fig. 3, demonstrating that the present jump ESPT model in eqn(15) explains the T+T dissociations and thus $k_D = 5 \times 10^{10}$ s^{-1} is concluded in the sequential ESPT model from Fig. 7.

From the time dependences of these contributions, the purple signals deactivate quicker than the green signals. This is rationalized by the faster spin-lattice relaxation caused by fluctuations in the ZFS interaction through the diffusion motion in T+T to induce the rotation of the ZFS principal axes in the disordered region (Fig. 2a). Note that the ZFS principal axes will be unchanged by the quick triplet exciton diffusion in the ordered region of Fig. 2b, resulting in long spin-lattice relaxation time in T+T for the green spectrum contribution.

3. Sequential electron spin polarization transfer model by the stepwise ^{1}TT → T···T → T+T dissociation

From Fig. 6 in the main text, the following coupled stochastic-Liouville equation can be obtained in the quintet (Q_l)-singlet (S) basis system where l = +2, +1, 0, -1 and -2, assuming that the quintet-triplet and the singlet-triplet interconversions are ignored.

$$\dot{\boldsymbol{\rho}}_{\mathbf{A}} = -i\left[\begin{pmatrix} E_{Q_l} & 0 \\ 0 & E_S \end{pmatrix}, \boldsymbol{\rho}_{\mathbf{A}}\right] - k_{\mathrm{J}}\boldsymbol{\rho}_{\mathbf{A}} \quad \text{(S1)}$$

$$\dot{\boldsymbol{\rho}}_{\mathbf{B}} = -i\left[\begin{pmatrix} H_{Q_lQ_l} & H_{Q_lS} \\ H_{SQ_l} & H_{SS} \end{pmatrix}, \boldsymbol{\rho}_{\mathbf{B}}\right] + k_{\mathrm{J}}\boldsymbol{\rho}_{\mathbf{A}} - k_{\mathrm{D}}\boldsymbol{\rho}_{\mathbf{B}} \quad \text{(S2)}$$

where subscripts A and B denote the strongly-coupled TT site (J = –170 GHz) and the intermediate T···T site with J = -11 MHz, respectively. E_{Ql} and E_S are the eigenenegies in TT with J = –170 GHz. H_{QlQl}, H_{QlS}, H_{SQl} and H_{SS} are respective diagonal and off-diagonal terms of the spin Hamiltonian ($\boldsymbol{H}_{\mathrm{T\cdots T}}$) of the intermediate T···T with J = –11 MHz on the basis spin system in the TT state. $\theta_2 = 90°$ and $\phi_2 = -5°$ were considered with Dss = -190 MHz in the intermediate T···T state, as shown by the T···T geometry in Fig. S3 based upon the crystal structure of TIPS-Pn (CSD Entry: VOQBIM). The density matrices are thus represented for the Q_l - S two-level systems, as, follows.

$$\boldsymbol{\rho}_{\mathbf{A}} = \begin{pmatrix} \rho^{\mathrm{A}}_{Q_lQ_l} & \rho^{\mathrm{A}}_{Q_lS} \\ \rho^{\mathrm{A}}_{SQ_l} & \rho^{\mathrm{A}}_{SS} \end{pmatrix}, \qquad \boldsymbol{\rho}_{\mathbf{B}} = \begin{pmatrix} \rho^{\mathrm{B}}_{Q_lQ_l} & \rho^{\mathrm{B}}_{Q_lS} \\ \rho^{\mathrm{B}}_{SQ_l} & \rho^{\mathrm{B}}_{SS} \end{pmatrix} \quad \text{(S3)}$$

The time-differential equation for the density matrix $\boldsymbol{\rho}^{\mathrm{T+T}}$ of the T+T state was thus obtained on the basis functions of $|i\rangle$ (i = 1, 2, ···, 9) of the diagonalized T+T system, as follows,

$$\dot{\boldsymbol{\rho}}^{\mathrm{T+T}} = k_D \, {}^{\mathrm{t}}\boldsymbol{U}_{\mathrm{T+T}}\boldsymbol{\rho}^{\mathrm{TT}}_{\mathrm{B}}\boldsymbol{U}_{\mathrm{T+T}} \quad \text{(S4)}$$

where

$$\boldsymbol{\rho}_B^{\mathrm{TT}} = \begin{pmatrix} \rho^{\mathrm{B}}_{Q_2Q_2} & 0 & 0 & & & & 0 & 0 & \rho^{\mathrm{B}}_{Q_2S} \\ 0 & \rho^{\mathrm{B}}_{Q_1Q_1} & 0 & & \square & & 0 & 0 & \rho^{\mathrm{B}}_{Q_1S} \\ 0 & 0 & \rho^{\mathrm{B}}_{Q_0Q_0} & & & & 0 & 0 & \rho^{\mathrm{B}}_{Q_0S} \\ & & & \rho^{\mathrm{B}}_{Q_{-1}Q_{-1}} & 0 & 0 & 0 & 0 & \rho^{\mathrm{B}}_{Q_{-1}S} \\ & \square & & 0 & \rho^{\mathrm{B}}_{Q_{-2}Q_{-2}} & 0 & 0 & 0 & \rho^{\mathrm{B}}_{Q_{-2}S} \\ & & & 0 & 0 & 0 & 0 & 0 & 0 \\ 0 & 0 & 0 & 0 & 0 & 0 & 0 & 0 & 0 \\ 0 & 0 & 0 & 0 & 0 & 0 & 0 & 0 & 0 \\ \rho^{\mathrm{B}}_{SQ_2} & \rho^{\mathrm{B}}_{SQ_1} & \rho^{\mathrm{B}}_{SQ_0} & \rho^{\mathrm{B}}_{SQ_{-1}} & \rho^{\mathrm{B}}_{SQ_{-2}} & 0 & 0 & 0 & \Sigma_j \rho^{\mathrm{B}}_{SS_{\square}} \end{pmatrix} \quad \text{(S5)}$$

We solved the time differential coupled equations (eqn S1, S2, S4 and S5) to obtain the diagonal elements ($\boldsymbol{\rho}^{\mathrm{T+T}}{}_{\mathrm{ii}}$ in eqn13) at t = 100 ns with the initial conditions of ρ^{A}_{SS}= 1 for each quintet ($\mathrm{Q_i}$)-singlet (S) two-level system with l = +2, +1, 0, -1 and -2. These nine diagonal elements were used to compute the EPR line-shapes using eqn(13).

We also examined the J-value effect on the computed EPR spectrum in the intermediate T···T state. However, we were unable to reproduce the green spectrum shape in Fig. 7 for any k_{D} value when $|J| > 20$ MHz was adopted instead of $J = -11$ MHz. In Fig. S3, the centre-to-centre separation distance between the TIPS-Pc molecules is estimated to be 0.8 nm. This larger T···T separation than the π-stacking separation of 0.34 nm for the cofacial TT may significantly weaken the exchange coupling from the GHz range to the MHz region. This is also consistent with the treatment that the attenuation factor of γ (= 1.7 $\mathrm{Å^{-1}}$) is large for the through-space electronic coupling as described by $V(r) = V_0 e^{-\gamma(r-d)}$ in the Pathways Model reported by Beratan (J. J. Regan, S. M. Risser, D. N. Beratan and J. N. Onuchic, *J. Phys. Chem.*, 1993, 97, 13083-13088.). Therefore, $J = -11$ MHz is a reasonable exchange parameter in the T···T state in the crystalline region.

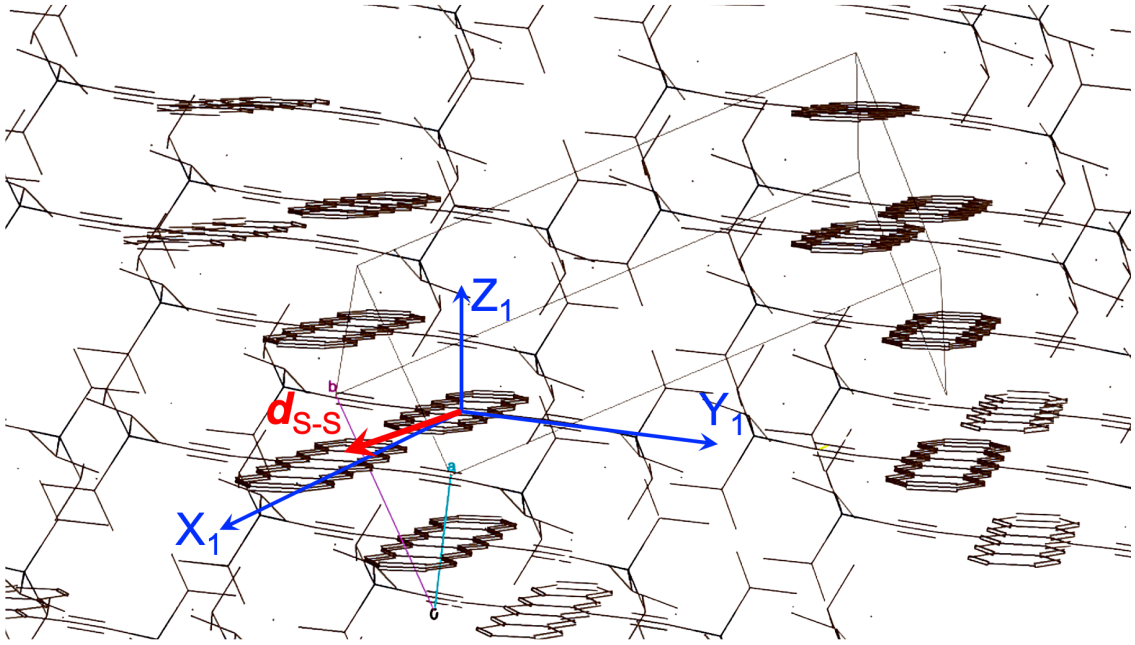

Fig. S3. Geometry of the intermediate T···T state considered for the present sequential ESPT model calculations (Fig. 7) from the crystal structure of TIPS-Pc (CSD Entry: VOQBIM). The second triplet exciton was assumed to be located at the polar angles of $\theta_2 = 90°$ and $\phi_2 = -5°$with respect to the principal axes (X_1, Y_1, Z_1) of the $\boldsymbol{D}_1$ tensor. $\boldsymbol{d}_{S\text{-}S}$ denotes the inter-spin vector between the triplet excitons, representing the principal axis of the spin-dipolar coupling. From Dss = -190 MHz, the inter-spin separation distance is estimated to be 0.75 nm in the intermediate T···T state.